Towards the use of the coccolith vital effects in palaeoceanography: A field investigation during the middle Miocene in the SW Pacific Ocean

Michaël Hermoso, Harry-Luke O Mcclelland, James S Hirst, Fabrice Minoletti, Magali Bonifacie, Rosalind E M Rickaby

Towards the use of the coccolith vital effects in palaeoceanography: A field investigation during the middle Miocene in the SW Pacific Ocean

Michaël Hermoso[a,b], Harry-Luke O. McClelland[c], James S. Hirst[d], Fabrice Minoletti[b], Magali Bonifacie[e], and Rosalind E. M. Rickaby[d]

[a] Université du Littoral Côte d'Opale, Université de Lille, CNRS, Laboratoire d'Océanologie et de Géosciences (UMR 8187 LOG), 62930 Wimereux, France.
[b] Sorbonne Université, CNRS, Institut des Sciences de la Terre de Paris (UMR 7193 ISTeP), 75005 Paris, France.
[c] Weizmann Institute of Science, Earth and Planetary Science Department, Rehovot, Israel.
[d] University of Oxford, Department of Earth Sciences, Oxford OX1 3AN, United Kingdom.
[e] Université de Paris, Institut de physique du globe de Paris, CNRS, 75005 Paris, France.

Corresponding author: Michaël Hermoso (michael.hermoso@univ-littoral.fr)

Highlights

- Size-specific carbon and oxygen isotopes are reported for coccoliths spanning the Miocene Climatic Transition (MCT)
- Coccoliths in different size classes show contrasting vital effects which are evaluated within an existing pCO_2 framework
- The observed correlation in $\Delta^{18}O/\Delta^{13}C$ between small and large species may reflect a decline in CO_2 through the MCT

Keywords: Coccoliths; Vital Effect; SST; pCO_2; Miocene; DSDP site 588

Abstract

Recent culture studies of living coccolithophores have established a biogeochemical framework for the use of the geochemical compositions of their calcite biominerals as proxies in palaeoceanography. Yet, questions remain regarding the transferability of such experimental data to fossil coccoliths. Here we analysed the carbon and oxygen isotopic composition of Miocene coccoliths to assess the suitability of such data for reconstructing the past environment. We found that the oxygen isotopic compositions of the relatively small Noelaerhabdaceae coccoliths gathered in the 3-5 μm fractions appear to be a suitable material to derive temperatures after a correction for a constant vital offset of 0.8‰. The interpretation of the isotopic signal of the relatively large Coccolithales coccoliths (5-8 μm fractions) is more complex, but supports results from cultures. The expression of the carbon and oxygen vital effect in coccoliths appears to be limited during the so-called Miocene Climate Optimum (MCO), a period of relatively elevated atmospheric pCO_2. Subsequently, during the Miocene Climatic Transition (MCT; ~14 Ma), which saw a decline in pCO_2, large carbon and oxygen vital effects were expressed in coccolith calcite. This phenomenon predates the postulated "*Late Miocene Threshold*" by approximately 4 Ma, and cannot be reconciled as a temporally-synchronous nor localised feature. Furthermore, we observed a statistically significant correlation between the oxygen and carbon offsets of the small relative to large coccoliths (hence, the vital effect *per se*) that is likely linked to variations in atmospheric CO_2. This biogeochemical correlation further supports a forcing of the environment on the cellular physiology (growth rate and utilisation of intracellular carbon) and ultimately the magnitude of isotopic vital effects in fossil coccoliths.

1. Introduction

Calcareous remains of coccolithophores dominate many pelagic sediment sequences since the Cretaceous. Thus, geochemical analyses on bulk sediments or the fine fractions are expected to primarily convey a biogeochemical signal of the uppermost water mass of the oceans where the coccolithophores calcify. Multiple papers have demonstrated that variations in bulk carbonate stable isotope records correlate in time across widespread locations and primarily represent the composition of coccoliths (Bolton et al., 2012; Bolton and Stoll, 2013; Hermoso, 2016; Reghellin et al., 2015; Rickaby et al., 2007; Rousselle et al., 2013; Tremblin et al., 2016). However, the magnitude of these variations differs among sampling sites, as well as between the foraminiferal and coccolith components of these records. These discrepancies are likely the results of large and variable expression of vital effects in coccolith calcite, which have limited the use of this climatic archive compared to the foraminifera (e.g., which assume small and constant vital effects).

Since the early work by Dudley et al. (1986), the origin of the isotopic vital effects in coccoliths has remained elusive. However, recent experimental and modelling work has enabled significant advances in our understanding of the causes underlying biological fractionation (Bolton and Stoll, 2013; Hermoso, 2014;2015;2016; Hermoso et al., 2015; 2016a; Hermoso and Lecasble, 2018; Holtz et al., 2015; McClelland et al., 2017; Minoletti et al., 2014; Rickaby et al., 2010; Ziveri et al., 2012). Specifically, it has emerged from these culture studies that the availability of ambient dissolved inorganic carbon (DIC) for the cells can significantly influence and modulate coccolith calcite $\delta^{18}O$ and $\delta^{13}C$ values, beyond expectations from ambient seawater composition and temperature alone. Culture studies by Rickaby *et al.* (2010) and Hermoso *et al.* (2016a) showed that the magnitude of the isotopic vital effects was variable in coccolith calcite, and overall, linked to pCO_2. The same finding was also deduced from stable isotope measurements of coccoliths in marine sediment cores (Bolton and Stoll, 2013). Meanwhile, the environmental forcing on the expression of the isotopic vital effects is not uniform among examined species, nor between the stable isotope systems. For the oxygen isotope system, the balance between ambient $CO_{2\,aq}$ concentration and intracellular utilisation dictates, to first order, the state of disequilibrium of the DIC–H_2O system when intracellular calcification occurs, and therefore the magnitude of the oxygen isotope vital effect (Hermoso et al., 2014; 2016b). This biogeochemical feature has direct implications for how fossil coccoliths have recorded ancient sea surface temperatures (SSTs). For the carbon isotope system, the expression of the vital effects derives from how cellular demand for carbon is met by cellular supply (Bolton and Stoll, 2013; McClelland et al., 2017). In addition to ambient carbon ($CO_{2\,aq}$) concentration, the cellular growth rate, the relative allocation of carbon into photosynthesis relative to calcification, and cell volume collectively dictate the magnitude of the carbon isotope vital effects. From a palaeoceanographic perspective, all of these parameters are difficult to assess from the fossil record.

Using the relatively well-constrained palaeoenvironmental framework available for the middle Miocene between ~17 and ~11 Ma, this work will examine the coherency of the coccolith record with foraminiferal data and independent pCO_2 estimates. The microseparation of sediments allows dissecting the geochemical complexity of marine deposits, as sediments are composed of a mixture of various micro- and nannofossils, as well as diagenetic particles. All these particles convey specific geochemical signals thought to reflect the environment from which they precipitate. In the case of the calcareous nannofossils, the micro-sized separation of the sediments offers the possibility to examine

how distinct size fractions compare in terms of their isotopic compositions. We are particularly interested in how environmental forcing can lead to distinct vital effects in different coccolith micro-assemblages (differing in taxonomy and size). Overall, our aim here is to establish how the isotopic composition of coccoliths can yield reliable climatic signals in light of recent constraints on the biogeochemical understanding of the vital effects.

## 2. Palaeoceanography of the middle Miocene

The Miocene is an Epoch typified by the transition from greenhouse to icehouse conditions of the Cenozoic (Lear et al., 2000; Zachos et al., 2001). The middle Miocene interval corresponds to a period of relative climatic instability, which represents an ideal case study to assess the magnitude of the vital effects in ancient coccoliths in response to climate forcing. A 12-Myr-long period of re-establishment of warmth culminated in the Miocene Climatic Optimum (MCO) between 17 and 14 Ma (**Fig. 1**). The MCO also corresponded to a period of disturbance of the isotopic carbon cycle (fluctuations of carbonate $\delta^{13}C$ values) with the so-called Monterey Event represented by a series of carbon maxima (CM) in the $\delta^{13}C$ profiles (Diester-Haass et al., 2013; Flower and Kennett, 1993; Vincent and Berger, 1985; Woodruff and Savin, 1991) (Fig. 1b). The termination of the MCO and the re-establishment of Cenozoic cooling occurred with a phase of sudden climatic transition, the Miocene Climatic Transition (MCT) between 14.8 and 15.2 Ma (Billups and Schrag, 2002; Lear et al., 2000; Shevenell et al., 2008) (Fig. 1). A compilation of existing atmospheric pCO$_2$ estimates for the investigated time slice, which is shown in Fig. 1c, indicates a relatively wide spread of values, from 200 to 500 ppm according to the considered study (Badger et al., 2013; Hollis et al., 2019; Kürschner et al., 2008; Zhang et al., 2013). Collectively, these pCO$_2$ estimates agree on decreased values across the MCT and the termination of the MCO. After this period of climate change (also supported by reconstructed seawater $\delta^{18}O$ values), atmospheric CO$_2$ levels appear to be relatively constant, at around 250-300 ppm. It is worth noting that boron isotope-derived pCO$_2$ estimates (Foster et al., 2012; Greenop et al., 2014) provide much more complex signals for this time slice and have therefore not been included in this compilation.

3. Material and Methods

3.1. Description of site 588

The chosen location for this sedimentary study is DSDP site 588 recovered on the Lord Howe Rise (26° South) in the Tasman Sea (**Fig. 2**). Reconstruction indicates a palaeolatitude of 32.2° South for this site (van Hinsbergen et al., 2015). The sediments used in the present study were recovered from the cores A and C and predominantly correspond to calcareous nannofossil oozes (Flower and Kennett, 1993; Kennett, 1986). The age model used for holes 588A and C is from the study by Holbourn et al. (2007) using the geological timescale 2004. Oldest datasets were converted for their age using the ODSN website (http://www.odsn.de/cgi-bin/conv_ts.pl). These include available foraminiferal $\delta^{18}O$ and $\delta^{13}C$ records including the surface-dweller *Globigerinoides quadrilobatus* and the epifaunal benthic *Cibicidoides* sp.. These foraminiferal data are from the high-resolution studies by Kennett et al. (1985) and Flower & Kennett (1993) across the 15.7 – 12.3 Ma interval (**Fig. 3**). More recent studies by Pagani et al. (1999, 2000), including measurements from the core 588C have extended the foraminiferal record to older and more recent sediments in the cores, thus providing a continuous record from 19.9 to 10.2 Ma. The ages of these complementary data were also converted to the GTS2004 using the ODSN website.

Hermoso et al. - Figure 1
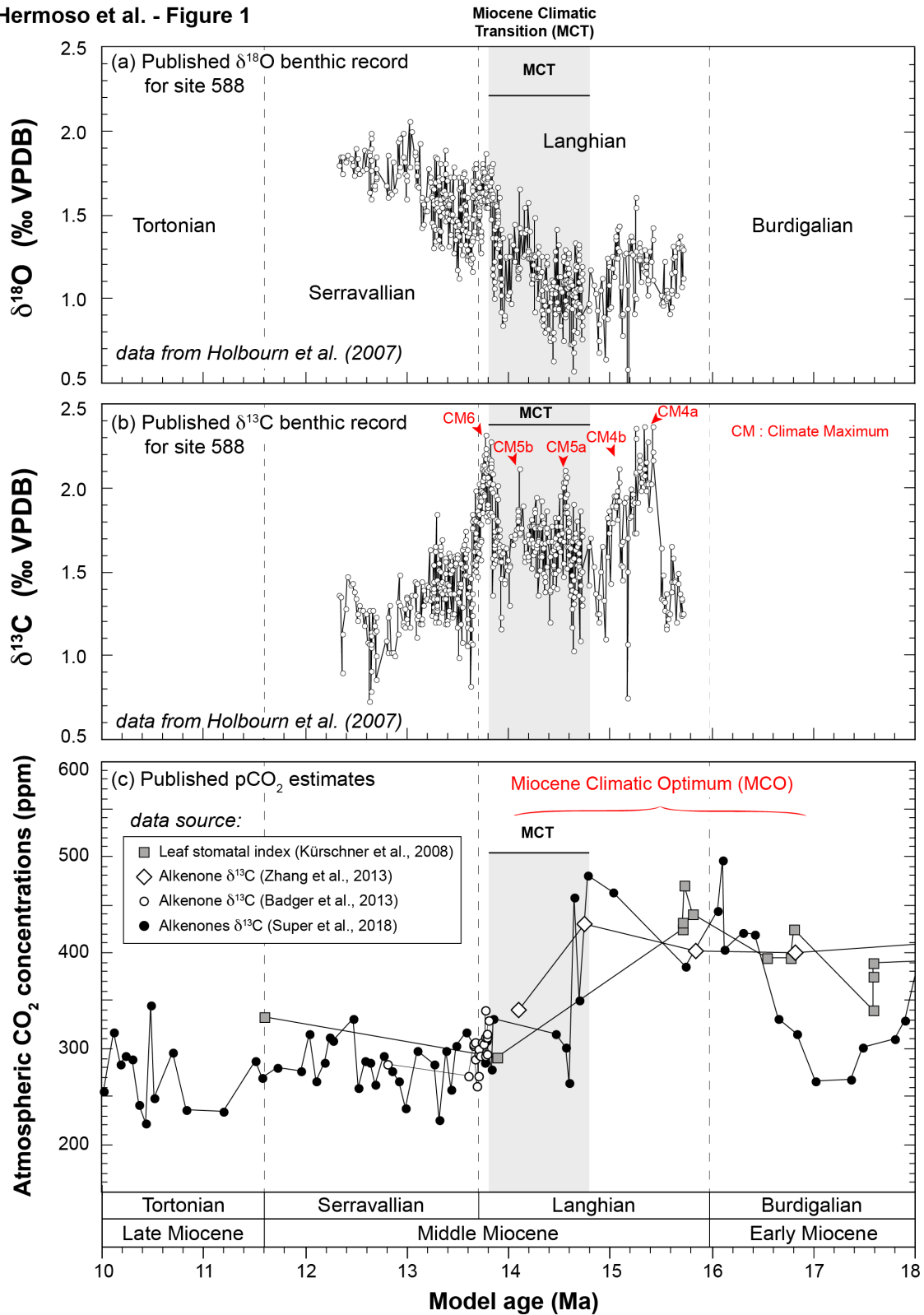
Figure 1. Oxygen and carbon isotope composition of benthic foraminifera for DSDP site 588 and atmospheric pCO₂ concentrations throughout the early to late Miocene. Panel a shows the available $\delta^{18}O$ benthic (*Cibicidoides* sp.) record for this site on which a shift towards more positive values is registered with the Miocene Climatic transition (MCT). Data source is inset. Panel b shows the coeval $\delta^{13}C$ benthic on which a series of (isotopic) carbon maxima (CM) –high $\delta^{13}C$ values– are recognised. They define the so-called Monterey carbon isotope excursion. Panel c depicts previously-reported pCO₂ estimates from various sources showing the array of reconstructed pCO₂ values. Overall, reported data are higher and variable during the MCO (~450 ppm) and a decrease is observed within the MCT and subsequently (~300 ppm). The data source for each curve is inset. For the errors associated to each published curve, please refer to the original publications.
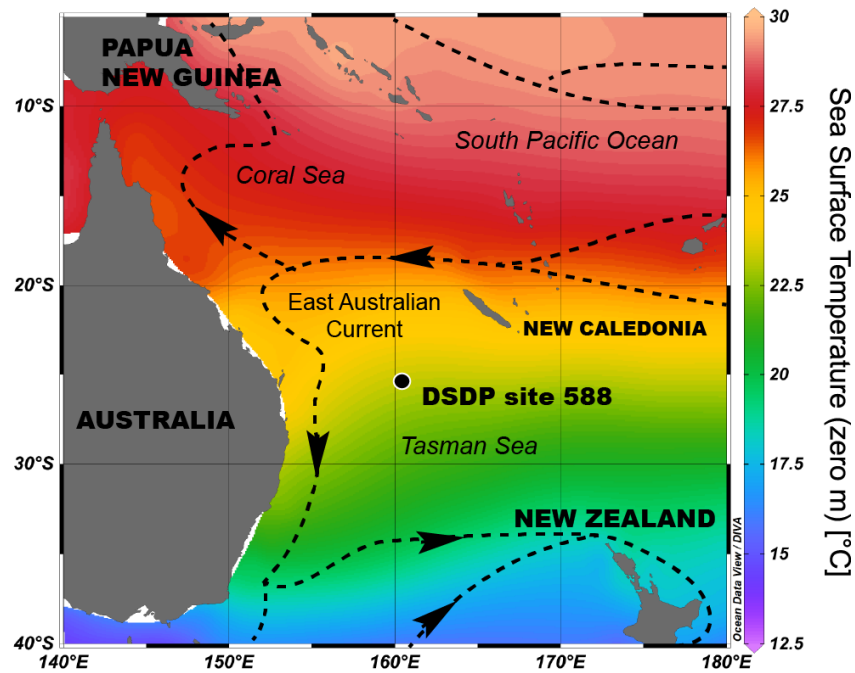
Figure 2. Location of the studied oceanic site in the Tasman Sea. The map layout was generated using Ocean Data View (Schlitzer, 2017). The surface currents (dashed lines with arrows) are from the figure 8.6 from Tomczak and Godfrey, 2003. The East Australian Current is a SW branch of the SW Pacific oceanic gyre flowing southward.

3.2. Coccolith microseparation

We applied the protocol of separation of coccoliths based on a cascade of microfiltering steps designed by Minoletti et al. (2009) where a full description of the method can be read. After dispersion and disaggregation of the sediment in neutralised deionised water using a gentle ultrasonic treatment for 10 minutes, the resulting suspension was wet sieved through 63 and 20 μm nylon mesh, steps that retained the coarse fraction comprising the foraminifera, large fragments and recalcitrant sediment aggregates. The <20 μm fractions were then processed using filtration columns and polycarbonate screen membranes with 12 μm; 8 μm; 5 μm and 3 μm nominal apertures.

All the presented microfractions have been examined under the optical and electron microscopes and checked for purity in terms of coccolith content. Under the light microscope, the 3-5 μm fractions contained calcareous assemblages that were almost exclusively composed of coccoliths dominantly belonging to the genus *Reticulofenestra* (Noelaerhabdaceae family). The adjacent coarser fractions, namely the 5-8 μm fractions, were more polyspecific, enriched in larger coccoliths of the *Coccolithus* group (Coccolithaceae family), but also containing variable abundances of *Calcidiscus* sp. coccoliths and *Discoaster* spp.. We did not make use of the isotopic composition of the <3 μm microfractions despite their richness in coccoliths, as they also contained appreciable amounts of the so-called micarbs whose nature (biogenic vs. diagenetic; allo- vs. autochtonous) remains undetermined (Beltran et al., 2009; Minoletti et al., 2009). Fractions that comprised less than 90 *wt*% of coccoliths were excluded from further analysis. Under the SEM, the coccoliths exhibited very good preservation with no notable overgrowth of calcite and only modest etching of the shields. This excellent preservation state, which was also noted for coeval foraminiferal shells (Flower and Kennett, 1993) is likely due to the

relatively shallow depositional depth with an approximately 1500-m-deep water column (present day value).

3.3. Isotopic measurements

The microfractions were measured for their oxygen and carbon isotope ratios using a VG Isogas Prism mass spectrometer at Oxford University. The size-separated fractions of the fractions were reacted with anhydrous H_3PO_4 at 90°C. Calibration to the V-PDB scale via NBS19 was made daily using the Oxford in-house Carrara marble standard. Reproducibility of replicated standards was usually better than 0.1‰ (±1σ) for $\delta^{18}O$ and $\delta^{13}C$.

We estimated the effect of a conservative 20*wt*% "contamination" of a considered microfraction from the two adjacent microfractions with a simple mass balance. On the example of the possible impurity of the 3-5 μm fractions, we imposed the presence of 10% of larger particles from the 5-8 μm fraction and 10% smaller from the <3 μm fraction to the 3-5 μm signals. This treatment was accounted for as numerically described in Eq. 1. The same calculation was conducted on the 5-8 μm fractions using the isotopic compositions of the bracketing 8-10 μm and 3-5 μm fractions.

$$Uncertainty\ on\ \delta_{3-5} = \delta_{3-5} \pm \left([0.8 \times \delta_{3-5}] + [0.1 \times \delta_{5-8}] + [0.1 \times \delta_{inf3}] \right) \quad \text{(Eq. 1)}$$

where the uncertainty of the isotopic composition "δ" in carbon or oxygen of the 3-5 μm fractions is in ‰ VPDB, as the individual measured isotopic ratios.

4. Results and discussion

4.1. Basic results

The coccolith $\delta^{18}O$ values range from -0.8‰ and +0.7‰ (**Fig. 3a**). We observe a progressive increase in this isotopic ratio over the studied interval, this long-term change matches the increase in reconstructed $\delta^{18}O_{sw}$ (**Fig. 3b**). Overall, the 3-5 μm and 5-8 μm fractions have close oxygen isotope compositions, especially prior to the MCT. During this transition, higher fluctuations between adjacent samples (3-5 μm and 5-8 μm fractions) become apparent, along with increased offset between the two coccolith microfractions – the $\delta^{18}O_{3-5\mu m}$ values being generally more positive by +0.4‰. The mean oxygen isotope composition of the coccoliths is shifted by +1.5‰ compared to their contemporaneous planktonic *G. quadrilobatus* foraminifera (**Fig. 3a**). The coccolith–foraminifera $\delta^{18}O$ offset tends to increase with time over the studied interval.

The absolute coccolith $\delta^{13}C$ values range from 0.9‰ and 2.7‰ (**Fig. 3c**). Although the resolution of the record is different between the two calcifiers, the Carbon Maxima defined from the planktonic foraminiferal record (**Fig. 1b**) can also be identified in the coccolith record. Before 12.4 Ma, we observe a good agreement between foraminifera and the coccolith fractions for their absolute $\delta^{13}C$ values (raw data), albeit with larger differences between the two type of biominerals between 14.2 and 14.8 Ma.

4.2. Frameworks for interpreting the results in terms of palaeoclimatic signals

4.2.1. Coccolith palaeo-vital effects from culture data

There are two ways to address the problem of the variable expression of the isotopic vital effect in sedimentary coccoliths. The first consists of quantifying the offset between size-restricted coccolith assemblages from a coeval, planktonic foraminiferal reference, as done in previous studies (Bolton et al., 2016; Bolton and Stoll, 2013; Hermoso, 2016). The second is to apply culture-derived biological offset correction to the isotopic signatures of different sized coccolith assemblages to account for the vital effect.

For the *a priori* treatment of the coccolith vital effect, we applied the biological offset correction accounting for the oxygen isotope vital effect (^{18}O VE) of cultured *Gephyrocapsa oceanica* to their Miocene close-relative *Reticulofenestra* coccoliths gathered in the 3-5 μm microfractions. Both taxa belong to the Noelaerhabdaceae family and have similar size. This offset correction (+0.8‰ VPDB) arises from the culture study by Rickaby et al. (2010). The oxygen isotope vital effect of *G. oceanica* is not sensitive to pCO_2 fluctuations ($pCO_2 > 280$ ppm) (Rickaby et al., 2010; Tremblin et al., 2016). We used the extreme values of the range of the culture data as a most conservative uncertainty of the fixed oxygen isotope vital effects (±0.1‰). Similar reconstruction of SSTs from *Reticulofenestra*-derived SSTs has been recently successfully applied across the Eocene–Oligocene Transition (Tremblin et al., 2016). Such a correction of the oxygen vital effect for the 5-8 μm microfractions is not as straightforward because the δ^{18}O / T relationship is more complicated than in smaller cells, and appears to be a function of CO_2 in larger coccoliths/cells (Bolton et al., 2016; Hermoso, 2014; Hermoso et al., 2020; McClelland et al., 2017; Rickaby et al., 2010; Tremblin et al., 2016; Ziveri et al., 2003). This explains why our coccolith δ^{18}O-derived SST curve only originates from the 3-5 μm microfractions (**Fig. 4**). Nevertheless, the δ^{18}O values of the 5-8 μm microfractions will be compared to the reticulofenestrid (3-5 μm fractions) and foraminifera records to shed light on the ^{18}O VE of ancient Coccolithales coccoliths (**Fig. 5**).

As outlined in the introduction, the drivers of carbon isotope vital effects are much more complex than for the oxygen isotope system (McClelland et al., 2017), and therefore, we did not attempt to correct the raw isotopic data for the coccoliths of the two microfractions. Nevertheless, the coccolith-foraminifera offsets ($\Delta^{13}C_{coccolith–foraminifera}$) will be presented and discussed (**Fig. 5**).

4.2.2. Ancient seawater δ^{18}O composition

Comparing δ^{18}O signals from the coccoliths to those from the foraminifera *per se* does not depend on assumed seawater oxygen isotope values ($\delta^{18}O_{sw}$), as it appears safe to assume that the coccolithophores and the foraminifera have built up their calcite shells from seawater with comparable δ^{18}O values. It becomes, however, necessary to make an assumption on the oxygen isotope composition of seawater in order to convert the oxygen isotope composition of fossil biogenic carbonates into temperature estimates (Eq. 2). Meanwhile, comparing the SSTs from the two biominerals will not be influenced by uncertainties in $\delta^{18}O_{sw}$ estimates.

Work by Flower & Kennett (1993) on the same study site did not attempt conversion of planktonic foraminifera δ^{18}O values into SSTs. Subsequent study by Pagani et al. (1999) used a relatively simple $\delta^{18}O_{sw}$ framework with a constant value of −1‰ and applied discrete positive steps on the order of several tenths of a per mil between 15 and 12 Ma when Antarctic ice-sheets were thought to have advanced (Flower and Kennett, 1993). In this study, we used the $\delta^{18}O_{sw}$ evolution documented by Lear et al. (2010) from ODP Site 761 that lies at a relatively close latitude to DSDP Site 588 (~16°S and ~26°S in present day,

respectively). Proxy data of bottom water $\delta^{18}O_{sw}$ inferred from the geochemistry of the benthic foraminifera *Oridorsalis umbonatus* (Lear et al., 2010) and modelling work enabled reconstruction of surface water $\delta^{18}O_{sw}$ values by Tindall & Haywood (2015) for a later time interval that showed relative homogeneity in bottom and surface $\delta^{18}O_{sw}$ values between the drilling locations of ODP site 761 and DSDP site 588 and provides support for the validity of the $\delta^{18}O_{sw}$ estimates from benthic foraminifera as an approximation of surface water $\delta^{18}O_{sw}$ (**Fig. 3b**).

4.2.3. Final $\delta^{18}O$ / Temperature equation accounting for the vital effect

The final temperature equation applied in the present study originates from the work by Kim & O'Neil (1997) and recast in the study by Tremblin et al. (2016) (Eq. 2). This equation contains three input parameters that are the oxygen isotope composition of coccolith calcite ($\delta^{18}O$), the treatment of the vital effect imprinting the composition of these biominerals (biological offset correction termed ^{18}O VE) and the isotopic composition of seawater ($\delta^{18}O_{sw}$).

$$SST = \frac{(1000 \times 18.03)}{(1000 \times \ln\,[(1000 + (1.03091 \times (\mathbf{\delta^{18}O} - \mathbf{^{18}O\ VE}) + 30.91))\,/\,(1000 + \mathbf{\delta^{18}O_{sw}})] + 32.17)} - 273.15 \qquad \text{(Eq. 2)}$$

where SST (Sea Surface Temperature) is in °C; both calcite $\delta^{18}O$ and oxygen isotope vital effects are in ‰ VPDB and $\delta^{18}O_{sw}$ is in ‰ VSMOW.

We must note that we were unable to associate an uncertainty with the $\delta^{18}O_{sw}$ parameter and to propagate it in the final temperature estimates. Due to the multiple assumptions made to generate these figures in the study by Lear et al. (2010) and subsequent work, it has indeed proven impossible to extract a typical error from the dataset. As we aim at comparing the foraminiferal and coccolith records from a palaeobiogeochemical perspective, and not using the SST, this has negligible effect on our discussion.

4.3. Confronting the various $\delta^{18}O$-derived temperature signals

4.3.1. SSTs derived from planktonic foraminifera and the "small" coccoliths (3-5 μm fractions)

Providing that the $\delta^{18}O$ values of surface-dwelling *G. quadrilobatus* record a signal of temperature with negligible oxygen isotope vital effect, as do those of modern *Globigerinoides* (Niebler et al., 1999; Pearson et al., 1997; Spero et al., 2003), it appears that SSTs derived from the $\delta^{18}O$ composition of coccoliths in the 3-5 μm microfractions containing *Reticulofenestra* spp. and corrected for a +0.8‰ vital effect appear to be in good agreement both for the absolute temperatures (ranging from 16 to 24 °C) and trends (**Fig. 4**). Although several discrete datapoints of coincident coccolith and foraminifera slightly diverge across the MCT and during the early Serravallian, the overall consistency between these two sources is reassuring for how culture-derived ^{18}O VE offsets can be applied to the fossil record.
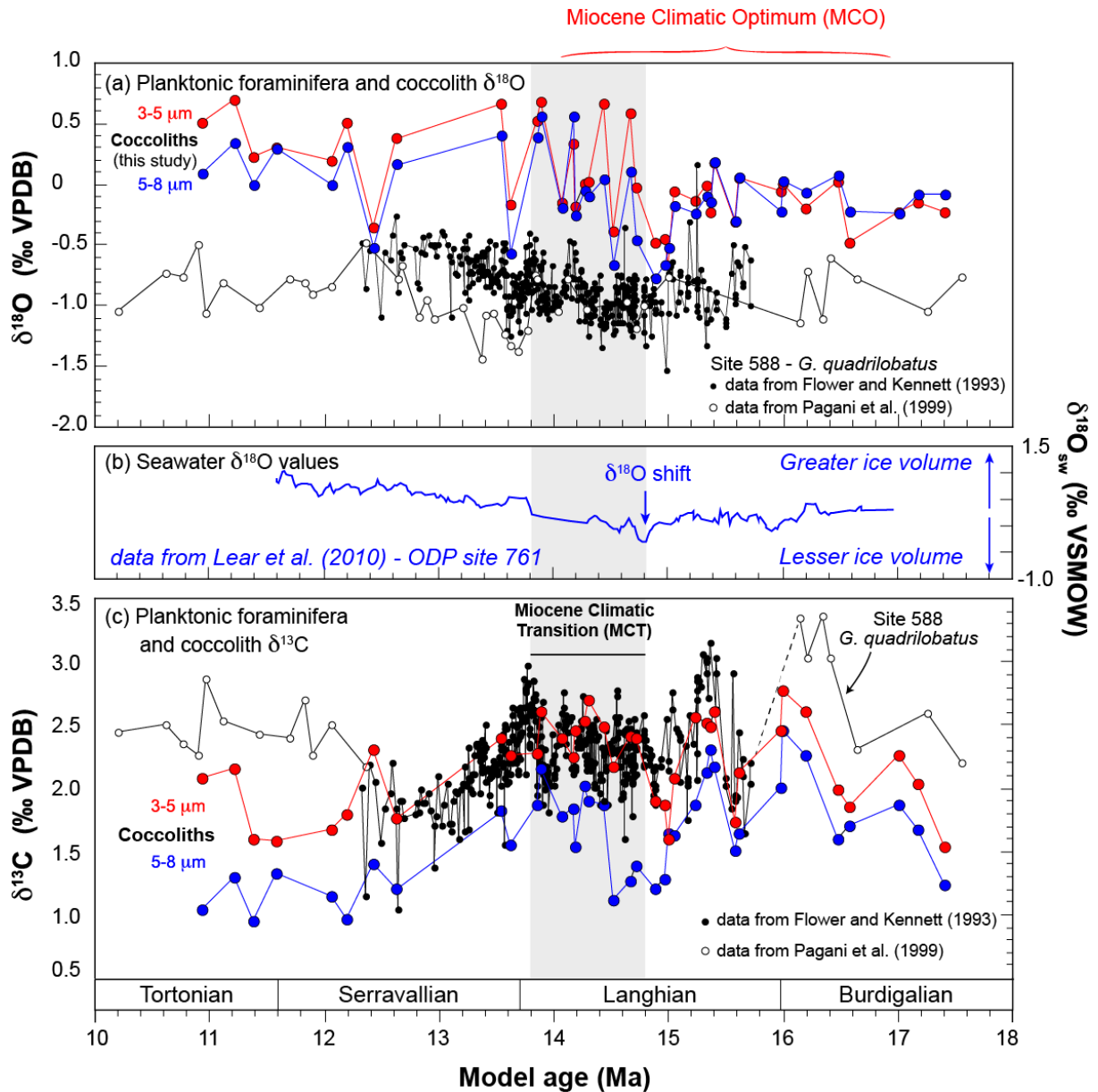
Figure 3. Raw oxygen and carbon isotopic composition of calcite biominerals (coccoliths and planktonic foraminifera). Panel a shows the evolution of oxygen isotope composition of planktonic foraminifera *G. quadrilobatus* (white and black dots) and the coccoliths of this study concentrated in narrow size microfractions throughout the studied interval (red and blue dots). The grey vertical area represents the interval of the middle Miocene Climatic Transition. Data source for the foraminifera measurements is inset. Panel b shows a reconstruction of $\delta^{18}O_{sw}$ across the study interval accounting from paired Mg/Ca and foraminifera $\delta^{18}O$ values. The correction of data accounts for changing CO_3^{2-} concentrations on the Mg/Ca calibration (data from Lear et al., 2010). We note that the onset on the MCT corresponds to a sharp increase in $\delta^{18}O_{sw}$ values. Panel c shows the evolution of carbon isotope composition of planktonic foraminifera and coccoliths. Data source is inset.

From a palaeoclimatic perspective, we only observe modest variations in SSTs at this location despite a relatively important decline in pCO_2 across the MCT. Although the record shows large variations between adjacent studied samples, the temperature decrease at this subtropical latitude can be quantified to approximately -2.5 °C from 17.4 to 13.5 Ma (**Fig. 4**), namely throughout the Miocene Climatic Optimum. Unlike other oceanic temperature records (e.g. Shevenell et al., 2004; Super et al., 2018), a warming phase is registered at the study site after the MCT. This event may seem out of place with the pCO_2 decline (**Fig. 1c**) and global climatic cooling (Zachos et al., 2001) (**Fig. 1c**; **Fig. 3b**). Previous studies have

suggested that this climatic event corresponds to a regional phenomenon caused by the reinforcement of the western boundary current of the south Pacific subtropical gyre (Flower and Kennett, 1993).

### 4.3.2. Examining the oxygen isotopic offsets between "small" and "large" coccoliths

The oxygen isotope composition of the large 5-8 μm fractions chiefly reflects those of the Coccolithales coccoliths (predominantly taxa within the *Coccolithus pelagicus* group). Some fractions also contain *Discoaster* nannoliths, these fractions were discarded from the dataset. The $\Delta^{18}O$ values between the 3-5 μm and 5-8 μm fractions ($\Delta^{18}O_{small-large}$) changed from –0.3 to +0.5 ‰ across the studied interval. No difference in preservation state was observed between the large and small reticulofenestrid coccoliths in the adjacent smaller microfractions. In the absence of deep-photic zone coccolith species in the microfractions, the taxa measured in the present study are thought to calcify at the same depth (Winter et al., 2002), so differences in ecology cannot be invoked to explain the difference between Coccolithales and Noelaerhabdaceae (reticulofenestrid) coccoliths. The large range of the oxygen isotope vital effect in larger coccoliths was expected, as they exhibit a much more complex biologically mediated fractionation (McClelland et al., 2017). To first order, the observed increase in $\Delta^{18}O_{small-large}$ indicates that the oxygen isotope vital effect of large coccoliths evolved with decreased pCO$_2$ values. This field observation supports our understanding from culture experiments of the biogeochemistry of large coccolithophore cells –*being more carbon limited with a smaller surface area-to-volume ratio*– and for which the expression of the vital effect is therefore more sensitive to ambient carbon limitation than small cells. We must note that this relationship between pCO$_2$ / CO$_{2\,aq}$ and vital effects is not resolvable by a detailed (peak to peak) observation throughout the entire record (**Fig. 3**). This is at least partly due to the large spread of existing data of pCO$_2$ for a given time interval. The co-variation between $\Delta^{18}O_{small-large}$ and $\Delta^{13}C_{small-large}$ offsets (**Fig. 6** and see following section 4.3) may shed light on factor(s) controlling this interspecies vital effect.

4.4. Coccolith carbon isotopes

#### 4.4.1. *Reticulofenestra* carbon isotope vital effects

Foraminifera *Globigerinoides quadrilobatus* and the coccoliths of the 3-5 μm fractions exhibit close $\delta^{13}C$ compositions, except from 12.4 Ma in the record where the coccoliths tend to be isotopically lighter (**Fig. 3c**). Applying a constant correction for the vital effect for *G. quadrilobatus* of +0.5 ‰ (by biogeochemical analogy of this species to *G. trilobus* (see work by Pearson et al. (1997)) leads the $\delta^{13}C$ values of the coccoliths to be isotopically lighter than the coeval planktonic foraminifera, inducing a "negative" carbon isotope vital effect (**Fig. 5a**). From 12.4 Ma, the vital effect in coccoliths becomes substantial, reaching 1.5 ‰. Recent biogeochemical modelling work points toward the importance of cell size, the degree of utilisation of the internal carbon pool and the PIC/POC ratios in coccolithophores to quantitatively describe coccolith $\delta^{13}C$ values (McClelland et al., 2017). Although these distinct mechanisms synergistically act on the carbon isotope vital effects, they are inter dependent and have been shown to be influenced by the concentration of ambient CO$_2$. The physiological parameters required to quantitatively explain the magnitudes of the vital effects in culture are difficult to assess from geological case studies, complicating the quantitative interpretation of the palaeo-vital effects. A way to move forward with the palaeobiogeochemical control of the ^{13}C VE is to acquire more data with precise quantification of the size and morphometrics of the coccoliths in the fractions (Bolton et al.,

2016; Duchamp-Alphonse et al., 2018; Hermoso and Minoletti, 2018; McClelland et al., 2016) and to generate independent seawater $\delta^{13}C_{DIC}$ and alkalinity estimates.
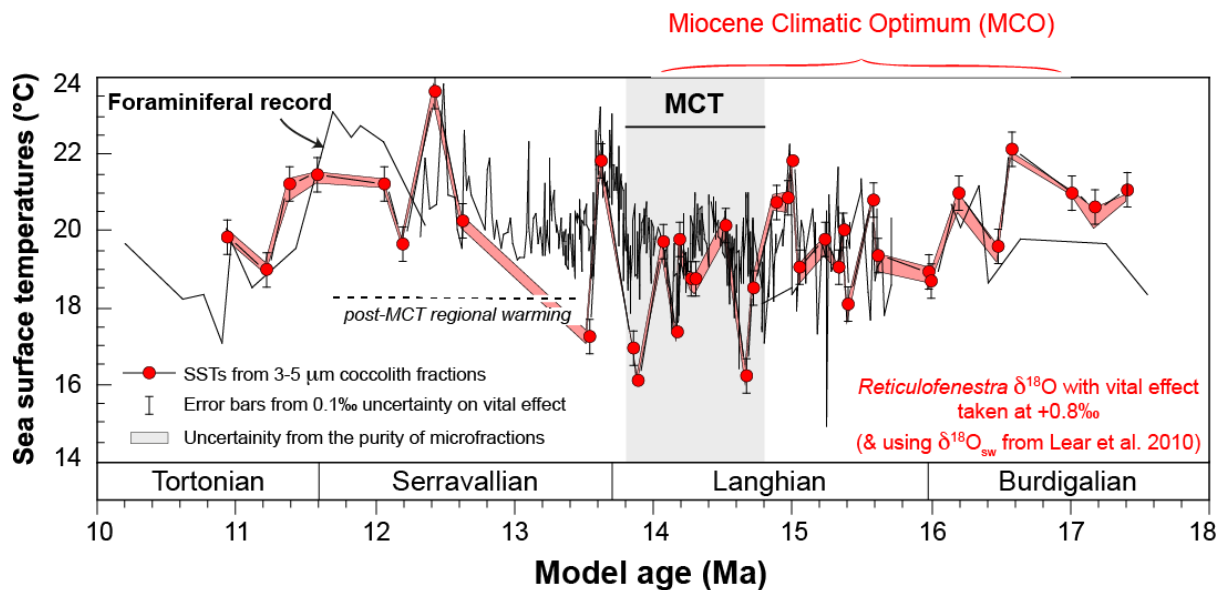
Figure 4. Comparison of sea surface temperature estimates derived from the oxygen isotope composition of foraminifera and coccoliths in the 3-5 μm microfractions. Both SST curved derived from Eq. 2 using the seawater $\delta^{18}O$ compositions shown in Fig. 3b. The coccolith (Reticulofenestrid) $\delta^{18}O$–derived SSTs at DSDP site 588 accounting for the culture-derived oxygen isotope vital effect for coccolith of this size range (0.8‰, see text) is in good agreement with the foraminiferal reference. Error bars on coccolith dots correspond to the uncertainties in the oxygen isotope vital effect (here taken at ±0.1‰). The pink area denotes a sensitivity test of the presence of 20wt% contamination by adjacent (coarser and finest) particles virtually pervading the 3-5 μm fractions on inferred SSTs.

The appearance of significant carbon isotope vital effects in relatively small cells may be caused by a decrease in pCO_2 through physiological changes related to carbon concentrating mechanisms (Bolton and Stoll, 2013) or simply through increased cellular utilisation of carbon (McClelland et al., 2017). Confronting this biogeochemical observation with the broader environmental context is not straightforward, as there is a large array of reconstructed pCO_2 values spanning the middle Miocene (**Fig. 1c**). However, our observations show that vital effects in coccolith calcite appeared some 4 Ma prior to the *CO₂ threshold* previously proposed by Bolton and Stoll (2013). The paper by Bolton and Stoll (2013) was the first to show a diversion in the magnitude of the small (3-5 μm fractions) vs. the large (5-8 μm fractions) coccolith $\delta^{13}C$ values that occurred during the late Miocene. Using simple numerical modelling, the authors argued that the decline in atmospheric pCO_2 was responsible for enhanced CO_2 limitation in large coccolithophore species, whereas the small ones, more permeable to ambient carbon due to a smaller cellular volume-to-surface area ratio, were still carbon replete and exhibited $\delta^{13}C$ ratios close to inorganic values. This discrepancy in the palaeobiogeochemical records either suggests that there are local effects at play (i.e., in the relationship between atmospheric pCO_2 and aqueous CO_2 concentration in seawater, in nutrient concentration and a possible change of growth rates caused by changing temperature) and/or that differential vital effects between large and small coccoliths truly appeared earlier than previously thought. In the future, further investigation, notably examining the evolution of coccolithophore size during this pivotal time interval, will help better understanding the global (biological) versus local (environmental) controls on stable isotope composition of coccolith calcite.
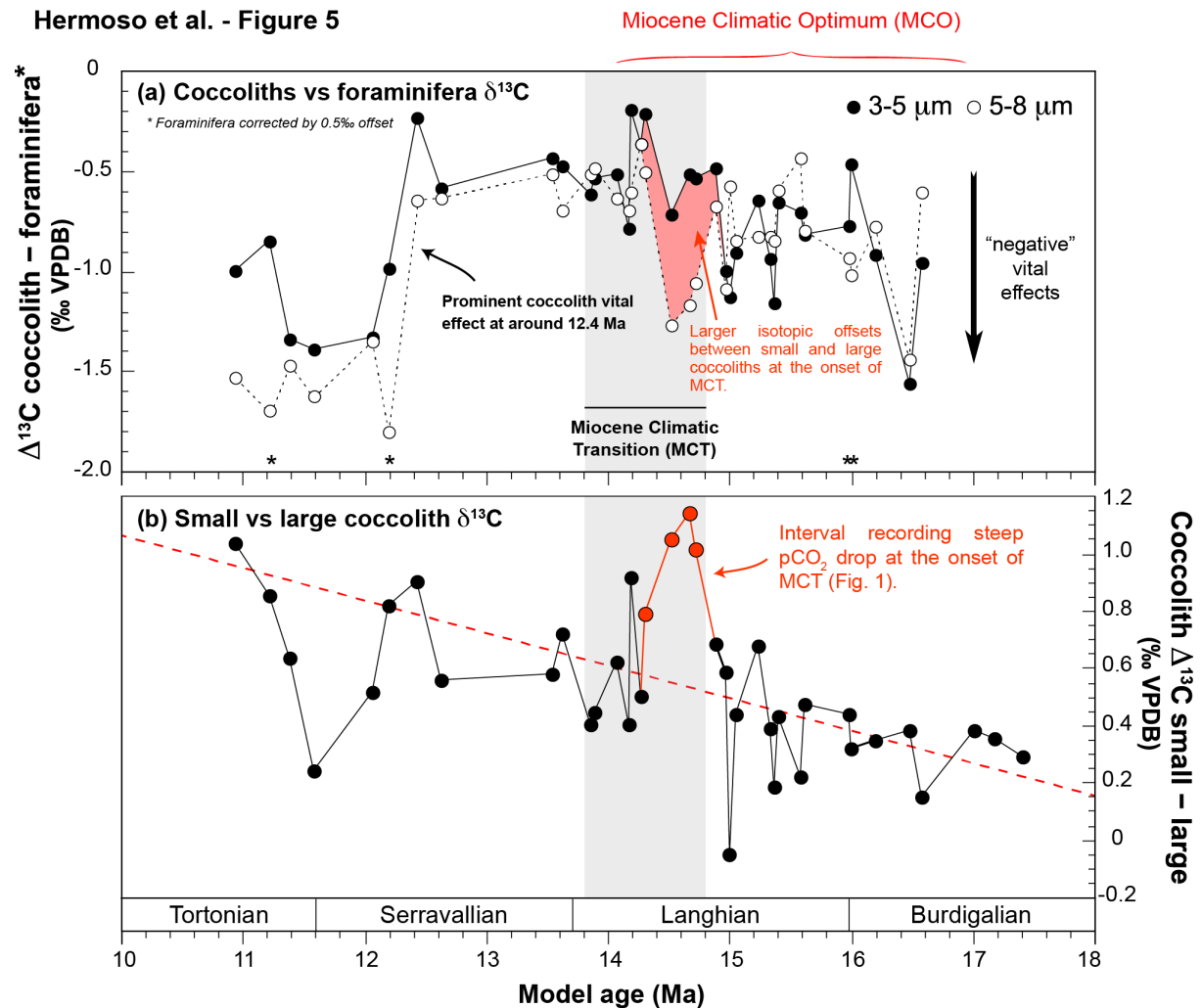
Figure 5. Expression of the carbon isotopic offsets between foraminifera and coccolith assemblages. Panel a compares $\delta^{13}C$ values of foraminifera (corrected by a ^{13}CVE factor of 0.5‰) with those of the coccolith assemblages (raw data). We observe enhanced negative carbon isotope vital effects at 12.5 Ma in the coccolith record. Asterisks denote levels that have require interpolation of foraminifera data. Panel b shows isotopic offset between coccolith fractions, comparable to the approach by Bolton & Stoll (2013) introducing "small–large" differences in the context of pCO$_2$ values (raw data). To first order, we observe progressive increased $\Delta^{13}C_{small–large}$ offsets across the studied interval that mirrors the decline in reconstructed pCO$_2$ values (Fig. 1c).

4.4.2. Differential expression of the vital effect by coccolith (cells) of contrasting sizes

The raw $\delta^{13}C$ values of the largest assemblages (5-8 μm fractions) are more negative than the small (3-5 μm fractions) ones by a mean offset of +0.55‰ (**Fig. 3c**). The uncertainties of the calculated $\Delta^{13}C$ values from the purity of the particles in the microfractions is less than 0.06‰ on average (see Methods). We note that in the record by Bolton & Stoll (2013), the carbon isotopic offset between the small *vs* large coccoliths between 18 and 10 Ma is also contained within a range of ±0.5‰. This overall good match between datasets, and presumably between microfractions containing distinct taxonomic assemblages, supports the observation of a generalisable feature of the biogeochemistry of the coccolithophores of a fixed size range during this time period.

The same prominent expression of the carbon isotope vital effect concerns the large coccoliths at 12.4 Ma (**Fig. 5a**). Prior to this event, there is decoupling of the expression of the vital effects between the small and large species that is apparent in our record at the onset

of the MCT (15.9 to 14.2 Ma) (depicted by the shaded pink zone on **Fig. 5a** and the red portion of the curve on **Fig. 5b**). At around 14 Ma in the record, the differential vital effects between the two assemblages vanished until the 12.4 Ma interval. The pCO_2 levels decreased across the MCT, also corresponding to the termination of the Monterey Event (a period of successive injections of CO_2 into the atmosphere). Thus, it can be inferred from this compilation of proxy data and with our incipient understanding of coccolithophore vital effects that ambient carbon concentrations declined across the studied interval. Our data pinpoint the advent of large vital effects imprinting coccolith calcite likely triggered by declining in the CO_2 resource required by the coccolithophores. Overall, the expression of the vital effect affecting coccolith calcite is confirmed here to be size dependent, as reported in culture studies.
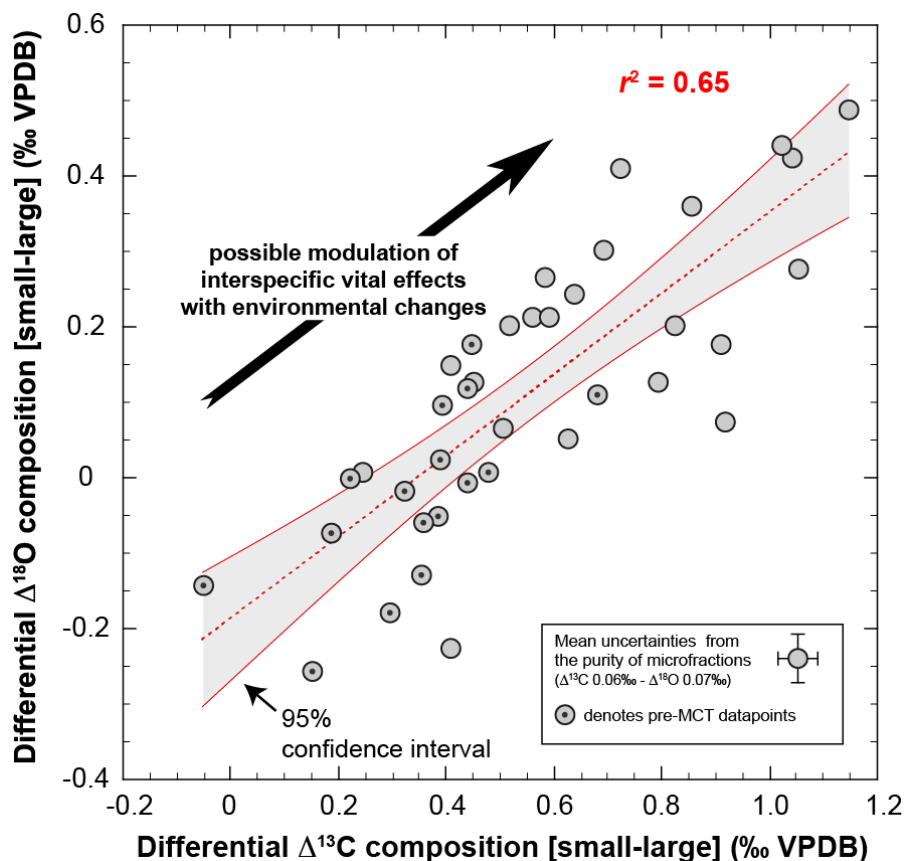
Figure 6. Scatter plot of the carbon and oxygen isotope compositions between relatively small and large coccolith assemblages. The data suggest that the vital effects affecting both carbon and oxygen isotopic systems are under a common environmental control, although the intracellular mechanisms at play differ (McClelland et al., 2017). The positive correlation conveys a biogeochemical signal that we hypothesize originates from a progressive decrease in aqueous CO_2 concentrations in seawater. The grey shaded area is the 95% confidence interval of the linear regression between $\Delta^{13}C$ and $\Delta^{18}O$ data.

4.5. On the potential the coccolith vital effects in palaeoceanographic research

The present study represents a step forward in the understanding of the environmental forcing of the isotopic composition of coccolith calcite, and their variation with time. A key observation is that that coccolith $\Delta^{13}C_{small–large}$ offsets positively correlate with $\Delta^{18}O_{small–large}$ values ($\delta^{18}O$ for smallest fraction uncorrected). This significant statistical link (p-value < 0.0005) is shown on **Fig. 6**. It is important to point out the lack of correlation between raw $\delta^{18}O$ and $\delta^{13}C$ for a given size fraction. Therefore, the differential expression of the vital effects in both isotopic systems must convey a primary biogeochemical signal. A pCO_2 driver

offers a likely explanation for the $\Delta^{18}O/\Delta^{13}C$ correlation, as the two isotopic systems were reported to be under a common control by $CO_{2\,aq}$ concentrations in laboratory-grown coccolith calcite (Hermoso et al., 2014). This observation was also found in a previous study of the geochemistry of subfossil coccolith laid on the seafloor to establish a core-top calibration of the stable isotope composition of the coccoliths with environmental parameters (Hermoso et al., 2015). Unfortunately for this study, it remains currently difficult to quantitatively explore the $\Delta^{18}O$ and $\Delta^{13}C$ figures with existing pCO_2 values, due to the relatively large array of reported pCO_2 values and uncertainties regarding ambient $CO_{2\,aq}$ concentrations. Further quantitative constraints on the forcing of seawater CO_2 concentrations and other environmental parameters on the expression of the carbon isotope vital effects among coccolith species could be possible, provided that independent estimates for growth rates and PIC/POC ratios are successfully obtained for deep time coccoliths (Gibbs et al., 2013; McClelland et al., 2016). In the future, developing a biogeochemically and environmentally grounded $\Delta^{18}O/\Delta^{13}O$ approach in culture and in sediments has the potential to resolve some uncertainties if the oxygen and carbon isotopes can be treated simultaneously through isotopic modelling.

5. Conclusions

This study provides a field validation of recent advances achieved through laboratory culture of coccolithophore species, and confirms the biogeochemistry of the coccolith as a valuable source of palaeoenvironmental information as a complement to the foraminiferal archive. In particular, this work unveils the intimate links between the carbon and oxygen vital effects and supports the hypothesis that their magnitude depends on the environment through the dynamics of CO_2 utilisation by the coccolithophore cells. Instead of being an obstacle to palaeoceanographic reconstructions, there is an increasing appreciation that coccolith vital effects themselves are rich in environmental information. It remains of utmost importance to better constrain the complexity of the coccolith biomineralising system by further laboratory cultures and an enhanced characterisation of the morphometrics of cultured and fossil coccoliths to establish a prospective paired $\Delta^{18}O/\Delta^{13}C$ proxy for ancient CO_2 concentrations.

Acknowledgments

Author contribution

M.H. designed to project. M.H., H.-L.M. and S.J. performed the experiments. All authors have contributed to the ideas presented in this study. M.H. wrote the paper with inputs from all co-authors.

References

Badger, M.P.S., Lear, C.H., Pancost, R.D., Foster, G.L., Bailey, T.R., Leng, M.J., Abels, H.A., 2013. CO$_2$ drawdown following the middle Miocene expansion of the Antarctic Ice Sheet. Paleoceanography 28, 42–53.

Beltran, C., de Rafélis, M., Person, A., Stalport, F., Renard, M., 2009. Multiproxy approach for determination of nature and origin of carbonate micro-particles so-called "micarb" in pelagic sediments. Sediment. Geol. 213, 64–76.

Billups, K., Schrag, D.P., 2002. Paleotemperatures and ice volume of the past 27 Myr revisited with paired Mg/Ca and ^{18}O/^{16}O measurements on benthic foraminifera. Paleoceanography 17, 1003.

Bolton, C.T., Hernández-Sánchez, M.T., Fuertes, M.-Á., González-Lemos, S., Abrevaya, L., Mendez-Vicente, A., Flores, J.-A., Probert, I., Giosan, L., Johnson, J., Stoll, H.M., 2016. Decrease in coccolithophore calcification and CO$_2$ since the middle Miocene. Nat. Commun. 7, 10284.

Bolton, C.T., Stoll, H.M., 2013. Late Miocene threshold response of marine algae to carbon dioxide limitation. Nature 500, 558–562.

Bolton, C.T., Stoll, H.M., Mendez-Vicente, A., 2012. Vital effects in coccolith calcite: Cenozoic climate- pCO$_2$ drove the diversity of carbon acquisition strategies in coccolithophores? Paleoceanography 27, PA4204.

Diester-Haass, L., Billups, K., Jacquemin, I., Emeis, K.C., Lefebvre, V., François, L., 2013. Paleoproductivity during the middle Miocene carbon isotope events: A data-model approach. Paleoceanography 28, 334–346.

Duchamp-Alphonse, S., Siani, G., Michel, E., Beaufort, L., Gally, Y., Jaccard, S.L., 2018. Enhanced ocean-atmosphere carbon partitioning via the carbonate counter pump during the last deglacial. Nat. Commun. 9, 1–10.

Dudley, W., Blackwelder, P., Brand, L., Duplessy, J.-C., 1986. Stable isotopic composition of coccoliths. Mar. Micropaleontol. 10, 1–8.

Flower, B.P., Kennett, J.P., 1993. Middle Miocene ocean-climate transition: High-resolution oxygen and carbon isotopic records from Deep Sea Drilling Project Site 588A, southwest Pacific. Paleoceanography 8, 811–843.

Foster, G.L., Lear, C.H., Rae, J.W.B., 2012. The evolution of pCO$_2$, ice volume and climate during the middle Miocene. Earth Planet. Sci. Lett. 341–344, 243–254.

Gibbs, S.J., Poulton, A.J., Bown, P.R., Daniels, C.J.,

Hopkins, J., Young, J.R., Jones, H.L., Thiemann, G.J., O'Dea, S. a., Newsam, C., 2013. Species-specific growth response of coccolithophores to Palaeocene–Eocene environmental change. Nat. Geosci. 6, 1–5.

Greenop, R., Foster, G.L., Wilson, P.A., Lear, C.H., 2014. Middle Miocene climate instability associated with high-amplitude CO$_2$ variability. Paleoceanography 29, 845–853.

Hermoso, M., 2016. Isotopic record of Pleistocene glacial/interglacial cycles in pelagic carbonates: Revisiting historical data from the Caribbean Sea. Quat. Sci. Rev. 137, 69–78.

Hermoso, M., 2015. Control of ambient pH on growth and stable isotopes in phytoplanktonic calcifying algae. Paleoceanography 30, PA002844.

Hermoso, M., 2014. Coccolith-derived isotopic proxies in palaeoceanography: Where geologists need biologists. Cryptogam. Algol. 35, 323–351.

Hermoso, M., Candelier, Y., Browning, T.J.T.J., Minoletti, F., 2015. Environmental control of the isotopic composition of subfossil coccolith calcite: Are laboratory culture data transferable to the natural environment? GeoResJ 7, 35–42.

Hermoso, M., Chan, I.Z.X., McClelland, H.L.O., Heureux, A.M.C., Rickaby, R.E.M., 2016a. Vanishing coccolith vital effects with alleviated carbon limitation. Biogeosciences 13, 301–312.

Hermoso, M., Horner, T.J., Minoletti, F., Rickaby, R.E.M., 2014. Constraints on the vital effect in coccolithophore and dinoflagellate calcite by oxygen isotopic modification of seawater. Geochim. Cosmochim. Acta 44, 612–627.

Hermoso, M., Lecasble, M., 2018. The effect of salinity on the biogeochemistry of the coccolithophores with implications for coccolith-based isotopic proxies. Biogeosciences 15, 6761–6772.

Hermoso, M., Minoletti, F., 2018. Mass and Fine-Scale Morphological Changes Induced by Changing Seawater pH in the Coccolith Gephyrocapsa oceanica. J. Geophys. Res. Biogeosciences 123, 2761–2774.

Hermoso, M., Minoletti, F., Aloisi, G., Bonifacie, M., McClelland, H.L.O., Labourdette, N., Renforth, P., Chaduteau, C., Rickaby, R.E.M., 2016b. An explanation for the ^{18}O excess in Noelaerhabdaceae coccolith calcite. Geochim. Cosmochim. Acta 189, 132–142.

Hermoso, M., Godbillot, C., Minoletti, F., 2020. Enhancing our palaeoceanographic toolbox using paired foraminiferal and coccolith calcite

measurements from pelagic sequences. Front. Earth Sci. 8:38. doi.org/10.3389/feart.2020.00038.

Holbourn, A., Kuhnt, W., Schulz, M., Flores, J.A., Andersen, N., 2007. Orbitally-paced climate evolution during the middle Miocene 'Monterey' carbon-isotope excursion. Earth Planet. Sci. Lett. 261, 534–550.

Hollis, C.J., et al., 2019. The DeepMIP contribution to PMIP4: methodologies for selection, compilation and analysis of latest Paleocene and early Eocene climate proxy data, incorporating version 0.1 of the DeepMIP database. Geosci. Model Dev. 12, 3149–3206.

Holtz, L.-M., Wolf-Gladrow, D., Thoms, S., 2015. Numerical cell model investigating cellular carbon fluxes in *Emiliania huxleyi*. J. Theor. Biol. 364, 305–315.

Kennett, J.P., 1986. Miocene to Early Pliocene Oxygen and Carbon Isotope Stratigraohy in the Southwest Pacific, Deep Sea Drilling Project Leg 90, Initial Reports of the Deep Sea Drilling Project.

Kennett, J.P., von der Borch, C., Baker, P.A., Barton, C.E., Boersma, A., Cauler, J.P., Dudley, W.C., Gardner, J. V., Jenkins, D.G., Lohman, W.H., Martini, E., Merrill, R.B., Morin, R., Nelson, C.S., Robert, C., Srinivasan, M.S., Stein, R., Takeuchi, A., Murphy, M.G., 1985. Palaeotectonic implications of increased late Eocene—early Oligocene volcanism from South Pacific DSDP sites. Nature 316, 507–511.

Kim, S.-T., O'Neil, J.R., 1997. Equilibrium and nonequilibrium oxygen isotope effects in synthetic carbonates. Geochim. Cosmochim. Acta 61, 3461–3475.

Kürschner, W.M., Kvaček, Z., Dilcher, D.L., 2008. The impact of Miocene atmospheric carbon dioxide fluctuations on climate and the evolution of terrestrial ecosystems. Proc. Natl. Acad. Sci. 105, 449–453.

Lear, C.H., Elderfield, H., Wilson, P.A., 2000. Cenozoic Deep-Sea Temperatures and Global Ice Volumes from Mg/Ca in Benthic Foraminiferal Calcite. Science 287, 269–272.

Lear, C.H., Mawbey, E.M., Rosenthal, Y., 2010. Cenozoic benthic foraminiferal Mg/Ca and Li/Ca records: Toward unlocking temperatures and saturation states. Paleoceanography 25, 1–11.

McClelland, H.L.O., Barbarin, N., Beaufort, L., Hermoso, M., Ferretti, P., Greaves, M., Rickaby, R.E.M.E.M., 2016. Calcification response of a key phytoplankton family to millennial-scale environmental change. Sci. Rep. 6, 34263.

McClelland, H.L.O., Bruggeman, J., Hermoso, M., Rickaby, R.E.M., 2017. The origin of carbon isotope vital effects in coccolith calcite. Nat. Commun. 8, 14511.

Minoletti, F., Hermoso, M., Candelier, Y., Probert, I., 2014. Calibration of stable isotope composition of Thoracosphaera heimii (dinoflagellate) calcite for reconstructing paleotemperatures in the intermediate photic zone. Paleoceanography 29, 1111–1126.

Minoletti, F., Hermoso, M., Gressier, V., 2009. Separation of sedimentary micron-sized particles for palaeoceanography and calcareous nannoplankton biogeochemistry. Nat. Protoc. 4, 14–24.

Niebler, H.-S., Hubberten, H.-W., Gersonde, R., 1999. Oxygen Isotope Values of Planktic Foraminifera: A Tool for the Reconstruction of Surface Water Stratification, in: Use of Proxies in Paleoceanography. Springer Berlin Heidelberg, Berlin, Heidelberg, pp. 165–189.

Pagani, M., Arthur, A., Freeman, H., 2000. Variations in Miocene phytoplankton growth rates in the southwest Atlantic: Evidence for changes in ocean circulation. Paleoceanography 15, 486–496.

Pagani, M., Arthur, M.A., Freeman, K.H., 1999. Miocene evolution of atmospheric carbon dioxide. Paleoceanography 14, 273–292. doi.org/10.1029/1999PA900006

Pearson, P.N., Shackleton, N.J., Hall, M.A., 1997. Stable isotopic evidence for the sympatric divergence of *Globigerinoides trilobus* and *Orbulina universa* (planktonic foraminifera). J. Geol. Soc. London. 154, 295–302.

Reghellin, D., Coxall, H.K., Dickens, G.R., Backman, J., 2015. Carbon and oxygen isotopes of bulk carbonate in sediment deposited beneath the eastern equatorial Pacific over the last 8 million years. Paleoceanography 30, 1–26.

Rickaby, R.E.M., Bard, E., Sonzogni, C., Rostek, F., Beaufort, L., Barker, S., Rees, G., Schrag, D.P., 2007. Coccolith chemistry reveals secular variations in the global ocean carbon cycle? Earth Planet. Sci. Lett. 253, 83–95.

Rickaby, R.E.M., Henderiks, J., Young, J.N., 2010. Perturbing phytoplankton: response and isotopic fractionation with changing carbonate chemistry in two coccolithophore species. Clim. Past 6, 771–785.

Rousselle, G., Beltran, C., Sicre, M.-A., Raffi, I., De Rafélis, M., 2013. Changes in sea-surface conditions in the Equatorial Pacific during the middle Miocene–Pliocene as inferred from coccolith geochemistry. Earth Planet. Sci. Lett. 361, 412–421.

Schlitzer, R., 2017. Ocean Data View Package. Available from: https://odv.awi.de.

Shevenell, A.E., Kennett, J.P., Lea, D.W., 2008. Middle Miocene ice sheet dynamics, deep-sea temperatures, and carbon cycling: A Southern Ocean perspective. Geochemistry, Geophys. Geosystems 9, Q02006.

Shevenell, A.E., Kennett, J.P., Lea, D.W., 2004. Middle Miocene Southern Ocean cooling and Antarctic cryosphere expansion. Science, 305, 1766–1770.

Spero, H.J., Mielke, K.M., Kalve, E.M., Lea, D.W., Pak, D.K., 2003. Multispecies approach to reconstructing eastern equatorial Pacific thermocline hydrography during the past 360 kyr. Paleoceanography 18, 2002PA000814.

Super, J.R., Thomas, E., Pagani, M., Huber, M., Brien, C.O., Hull, P.M., O'Brien, C., Hull, P.M., 2018. North Atlantic temperature and pCO$_2$ coupling in the early-middle Miocene. Geology 46, 519–522.

Tindall, J.C., Haywood, A.M., 2015. Modeling oxygen isotopes in the Pliocene: Large-scale features over the land and ocean. Paleoceanography 30, 1183–1201.

Tomczak, M., J Stuart Godfrey, 2003. Regional Oceanography: An Introduction. Daya Publishing House.

Tremblin, M., Hermoso, M., Minoletti, F., 2016.

Equatorial heat accumulation as a long-term trigger of permanent Antarctic ice-sheets during the Cenozoic. Proc. Natl. Acad. Sci. USA 113, 11782–11787.

van Hinsbergen, Douwe J. J. de Groot, L. V., van Schaik, S.J., Spakman, W., Bijl, P.K., Sluijs, A., Langereis, C.G., Brinkhuis, H., 2015. A Paleolatitude Calculator for Paleoclimate Studies (model version 1.2). PLoS One 10, 1–21.

Vincent, E., Berger, W.H., 1985. Carbon dioxide and polar cooling in the Miocene: The Monterey hypothesis, in: Sundquist E.T., Broecker, W.S. (Eds.), The Carbon Cycle and Atmospheric CO_2: Natural Variations Archean to Present. American Geophysical Union, pp. 455–468.

Winter, A., Rost, B., Hilbrecht, H., Elbrächter, M., 2002. Vertical and horizontal distribution of coccolithophores in the Caribbean Sea. Geo-Marine Lett. 22, 150–161.

Woodruff, F., Savin, S., 1991. Mid-Miocene isotope stratigraphy in the deep sea: High-resolution correlations, paleoclimatic cycles, and sediment preservation. Paleoceanography 6, 755–806.

Zachos, J., Pagani, M., Sloan, L., Thomas, E., Billups, K., 2001. Trends, rhythms, and aberrations in global climate 65 Ma to present. Science, 292, 686–693.

Zhang, Y.G., Pagani, M., Liu, Z., Bohaty, S.M., Deconto, R., 2013. A 40-million-year history of atmospheric CO_2. Philos. Trans. R. Soc. A 371, 20130096.

Ziveri, P., Stoll, H., Probert, I., Klaas, C., Geisen, M., Ganssen, G., Young, J., 2003. Stable isotope 'vital effects' in coccolith calcite. Earth Planet. Sci. Lett. 210, 137–149.

Ziveri, P., Thoms, S., Probert, I., Geisen, M., Langer, G., 2012. A universal carbonate effect on stable oxygen isotope ratios in unicellular planktonic calcifying organisms. Biogeosciences 9, 1025–1032.